Article

Optimization of Tillage Operation Parameters to Enhance Straw Incorporation in Rice-Wheat Rotation Field

Sagni B. Miressa [1,2], Qishuo Ding [1,*], Yinian Li [1] and Edwin O. Amisi [1]

[1] Key Laboratory of Intelligent Agricultural Equipment of Jiangsu Province, College of Engineering, Nanjing Agricultural University, Nanjing 210031, China; miressa5805@gmail.com (S.B.M.); edwineamisi@stu.njau.edu.cn (E.O.A.)

[2] Department Agricultural Engineering, School of Food and Agriculture Engineering, Hachalu Hundessa Campus, Ambo University, Ambo 25119, Shewa, Ethiopia

[*] Correspondence: qsding@njau.edu.cn

Abstract: In the rice-wheat system, using straw for soil incorporation provides better soil health and improves agricultural production. The experiment was performed in Babaiqiao town, Jiangsu Province, China's Luhe District, Nanjing City, in June 2024 using a Shichao TG-500 tractor equipped with a Qingxuan 1GKN-180 rotary cultivator. The impacts of the three tillage practices, deep rotary tiller with straw (DRTS), shallow rotary tiller with straw (SRTS), and no-tillage with straw return (NTSR), on the level of soil disturbance were observed in the single-factor and two-factor interaction experiments. Based on the profilometry analysis, it was observed that DRTS had the highest value of soil disturbance while SRTS had a moderate disturbance value and NTSR minimized disturbance. The effects of working depths, forward speed, and rotation speed on the straw return rate have been evaluated by further investigations. The results showed that enhancing straw return rates was significantly impacted by changing the tilling depths and the rotation speeds, especially when using deeper tillage and moderate to high rotary speeds. The investigation found that the forward speed, blade rotation speed, and tillage depth explained the overall rates of straw return, soil breaking, and soil flatness. In the research, the response surface design employed was the Box–Behnken Design (BBD). The optimal operating parameters were 14.23 cm of plowing depth, 297.6 rpm for the rotary blades, and 3.23 km/h for forward speed. Achieved were the following parameters: 94.766% soil breakage rate, 84.97% straw return rates, and 16.36 mm soil flatness. The findings demonstrate the potential to implement strategies through operational parameters to significantly enhance agricultural practices.

Keywords: profilometry; straw return; rotary tiller; soil disturbance; tillage depth

1. Introduction

A rice-wheat crop cultivation area, which is quite common in today's world agriculture, is also very essential for food stability and supports the rural people economically, especially in parts of the world like South Asia, as highlighted by [1,2]. This type of farming affords the farmer greater yield, reduces soil erosion, and improves soil fertility by incorporating straw or crop residues [3,4]. The use of tillage operations enables enhancement of the status of the soil in relation to the kinds of residue from the crops, preparing the soil for planting later [5,6]. Nevertheless, the major role of technological management of the tillage process is to evaluate the incorporation parameters of straw in rice-wheat rotation fields. Crop residues such as rice and wheat straw can be returned to the soil to increase the

organic matter content, pulp, and nutrient cycling, hence improving the overall health of the soil [6–8]. Tillage involves mixing straw into the soil, directly affecting soil fertility, nutrient cycling, and organic matter content [9,10]. Optimal tillage parameters while incorporating the maximum quantity of straw while at the same time preserving the soil and the efficiency of operations is a challenge. For increased straw incorporation in RW systems, researchers have been busy developing conservation tillage methods that can better help in the integration of straw into the soil [11,12]. The study has focused on various types of tillage, such as straw no-till, shallow rotary, and deep rotary with straw, to determine the extent of soil disturbance and straw return in the corn–wheat–corn sequence [13,14]. The results suggested that greater penetration depth and rotation rates deviating from moderate levels were necessary for the straw to thoroughly mix with the soil. Furthermore, the conclusions also pointed to the relevance of these types of tillage. Factors in straw return rates according to the results are described by [15,16]. Using these techniques would enable one to increase the proportion of organic matter in the soil and the capacity of the straw burial, which depends on the following parameters of the rotary blade, its rotational speed, forward speed, and cultivation depth [17–19]. However, to achieve the optimal soil breakage rate, effective straw incorporation, and ground flatness, the operating speed of the rotary tillage knife and the forward speed of the implement can be adjusted [20,21]. Tillage operation factors in rice-wheat rotation fields can be studied to enhance the incorporation of straw through the help of BBD and RSM [7,22]. Based on these techniques, it is possible to establish the interaction model of rotary blade soil and straw to identify the variables of power consumption and operation quality in deep rotary tillage and structural and operational parameters [7,23,24]. The factors that affect the tillage equipment can also be controlled in such a way that there will be efficient incorporation of the straw by applying BBD and RSM as espoused by [22,24]. The Box–Behnken response surface trials were conducted for every factor at three different levels in the optimization process. This enabled an assessment to be made depending on the blade's rotation speed and the extent of tilling required to produce the needed results. To determine the relationship and significance of the components and their relations, the study employed complex statistics like regression analysis and ANOVA. Considering the use of Design-Expert applications, 13.0, the data were used in the analysis for enhancement of the understanding of the optimum tillage conditions.

A thorough understanding of how to employ experimental designs and statistics to enhance tillage operation parameters for better straw mixing, soil breakdown rates, and flattening of the soil surface is needed. Consequently, the objective of this study is to determine the optimal tillage operation settings, which would also raise the rate of straw re-turn on the soil as well as the quality of the cover. Specifically, the influence of the tillage factors such as the speed of the tractor, the depth of tillage, and the speed of blade rotation for field application, are examined. This study focused on three specific parameters: for-ward speed, rotary blade speed, and the depth of the soil layer. We need to understand this since previous studies have aimed more at identifying the main effects rather than interactions of these traits. To enhance the straw incorporation into the rice-wheat systems, this paper seeks to calibrate the operating conditions of the Qingxuan 1GKN-180 rotary tiller. This study aims to achieve the following objectives: (i) utilize a profilometer for precise soil profile measurement and graphical representation to analyze the soil disturbance index; (ii) identify the optimal combination of tillage depth, blade rotational speed, and forward speed to maximize crop residue incorporation and enhance tillage quality; and (iii) validate the optimized parameters through field experiments. This research systematically examined tillage parameters, from which the approach to straw incorporation and soil management can be determined.

2. Materials and Methods

The field test was conducted in June 2024 in a typical tableland region located in Babaiqiao (118°59′ E, 31°98′ N), Luhe District, Nanjing, Jiangsu Province, China. The summer wheat crop field was subjected to a tillage test immediately following harvest. Rice and wheat have been rotated on the clay loam soils in the region. The measurements of the characteristics of the soil and straw are shown in Table 1.

Table 1. Experimental location factors for soil and straw.

Category	Factors	Value
Soil	Moisture content (0–30 cm)	15.4–28.6%
	Soil pH	6.5–7.8
	Dry bulk density	1.2–1.4 g/cm^3
	Cone Index (0–30 cm)	500–1745 kPa
	Nutrient levels: Nitrogen (N), Phosphorus (P) Potassium (K) (0–20 cm)	15–30, 21–36, 53–100 mg/kg respectively
Straw	Straw coverage	Evenly distributed
	Straw length	2–18 cm
	Straw density	4.377 kg/m^3
	Straw Dry density	3.493 kg/m^3

2.1. Description of Farming Tractors and Equipment

The equipment used in this study included a Qingxuan 1GKN-180 rotary tiller and a Shichao TG-500 tractor. The tractor was manufactured by Sichuan Shichao Agricultural Machinery Co., Ltd., located in Chengdu, Sichuan, China, while the rotary tiller was produced by Nanjing Agricultural Machinery Co., Ltd., based in Nanjing, China. The engagement was conducted with the help of a 45-HP Shichao TG-500 tractor. The engagement was conducted with the help of a 45-HP Shichao TG-500 tractor. The dimensions of the TG-500 are compact: Specifically, they measured 2300 mm in length, 1300 mm in width, and 900 mm in height and offer the ease of maneuvering in restricted areas and narrow corridors as well. It can be controlled in various areas and states, and you can shift through the 6 + 1 gears. This has grip from the rear wheels, which helps in providing stability on various surfaces while having the front track of 400 mm and rear wheel of 600 mm.

Straw was returned and mixed with soil using a 1GKN-180 rotary tiller during the field experiment. For rice-wheat stubble paddy fields, the 1GKN-180 rotary tiller is a popular choice because it outperforms other straw return equipment in terms of work stability. Table 2 displays the 1GKN-180 rotary tiller specifications.

Table 2. Brief specification of the study's related implementations.

Parameter	Specification
Type of Implement and Model	Rotary tiller and 1GKN-180
Standard ID	GB/T 5668-2017; Rotary Tiller and 1GKN-180. China: Beijing, China, 2017.
Weight (kg)	415
Power (hp)	36.8~44.1
Length × width × height (mm^3)	865 × 2090 × 1060
Maximum working depth (mm)	5–16 cm
Cultivation width (cm)	180
Number of blades	56
Blade model	IT225

2.1.1. Overall Structure and Main Parameters

The width, shaft length, and base thickness of the IT225 models' rotary tillage blade are 2300 mm, 200 mm, and 22 mm, respectively. When the blade shafts of two adjacent rotary tillers with a shared positive cutting edge revolve, a cylindrical form is created. The

62 mm gap between the center surfaces of the two tillers is determined by the operational width of the IT225 rotary tillage blade; this space should not be too large to prevent soil clamping [25,26]. Figure 1 depicts the general layout of the straw-returning apparatus. The gearbox frame, three-point suspension system, real axle returning cutter roller, and other parts make up the majority of the apparatus. Figure 1a depicts the 1GKN-180 rotary tiller structure. Figure 1b shows the IT225 rotary tiller blade, and Figure 1d illustrates the blade arrangement. The complete machine may change the working depth on the blade shafts in the rotary plow section by pulling a rod on the suspension frame.
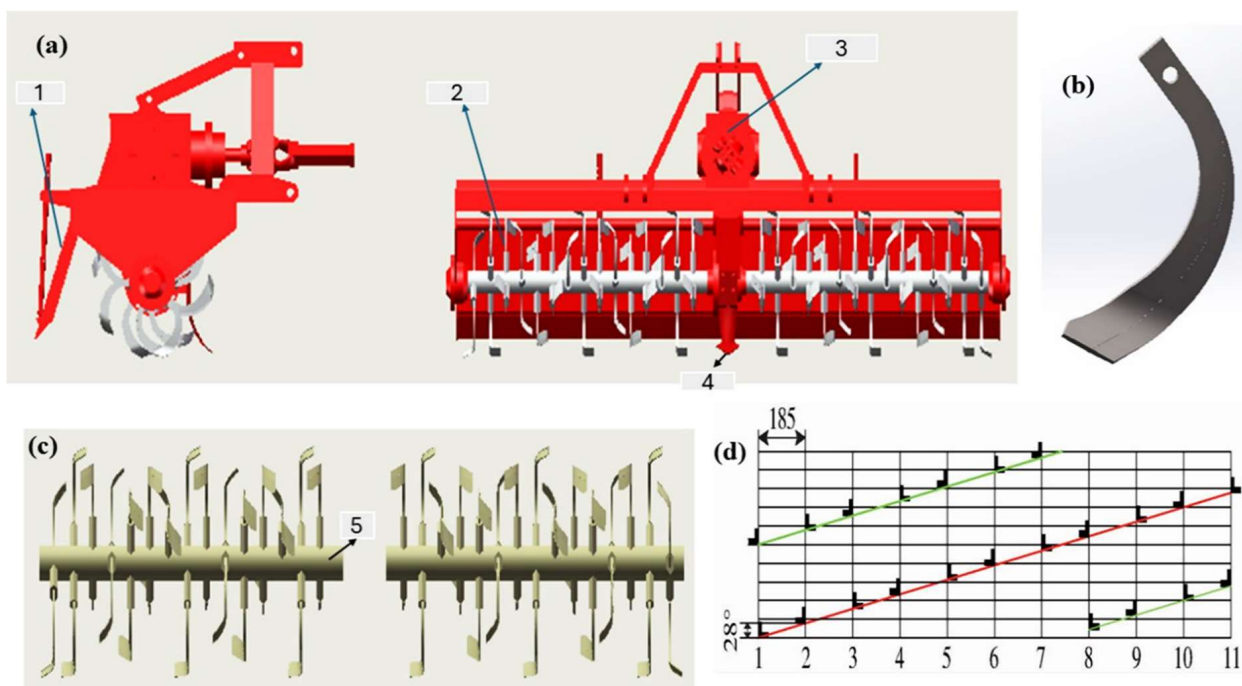

Figure 1. Structural diagram of the 1KGM-180 rotary tiller: 1. Fence, 2. Blade roller, 3. Transmission, 4. Furrow opener, 5. Knife seat. (**a**) 3D structure of rotary tillage; (**b**) IT255 rotary blade; (**c**) rotary tiller roller; (**d**) rotary blade arrangement.

2.1.2. Working Principle

For instance, in the case of the 1GKN-180 rotary tiller, a PTO (power take-off) shaft transfers the tractor's power to the 1GKN-180 rotary tiller gearbox to make it operational. With the help of this gearbox, the PTO's rotary motion generated here produces the horizontal rotary motion for the blades. This tiller has a horizontal rotor that comes with an IT255 blade. While rotating, these blades dig into the ground, scoop up the soil, and simultaneously break it into smaller, more manageable pieces. This movement, coupled with cultivation, also helps to make sure that there is an even distribution of organic matter in the soil and the eradication of weeds [27]. Operating depths may vary between 5 cm and 16 cm depending on the type of crop that is being cultivated or the state of the soil. The width of the tillers is 180 cm; this implies that huge areas are covered in one data pass. Figure 2 shows the visible characteristics of the model; the 1GKN-180 is an efficient and multifunctional soil preparation tool.
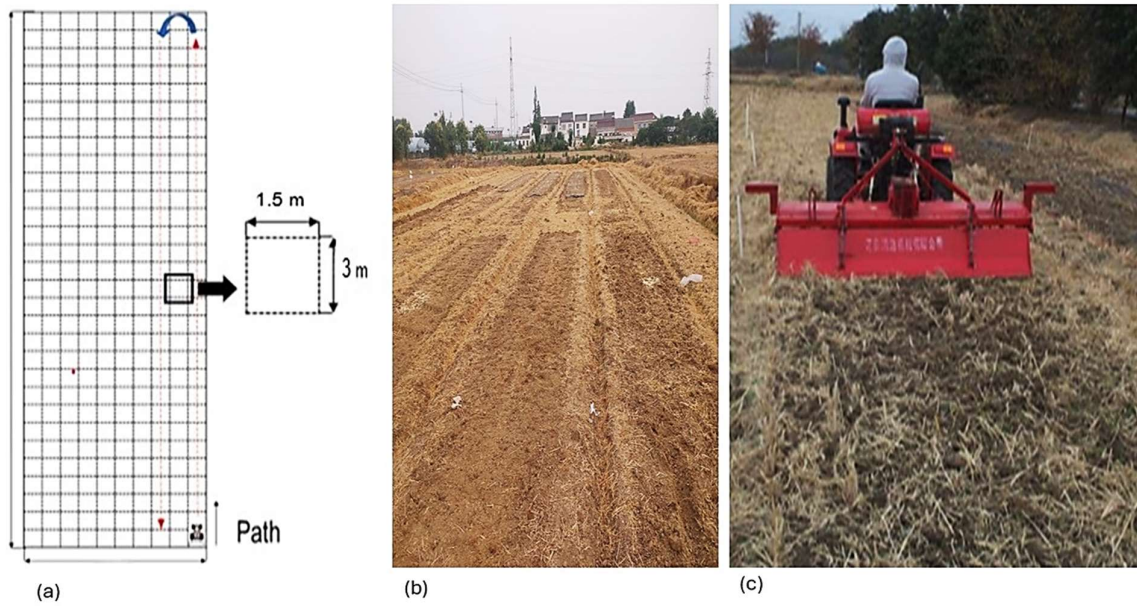
Figure 2. Experiment's trial area locations: (**a**) conceptual diagram of field grid separation; (**b**) the experiment field plot; (**c**) Shichao TG-500 tractor and Qingxuan 1 GKN-180 rotary tiller utilized in the field experiment.

2.1.3. Experimental Design and Treatment for Field Trials

Figure 3 depicts an experimental framework for assessing the tillage and straw management impact on soil parameters and operational efficiency.
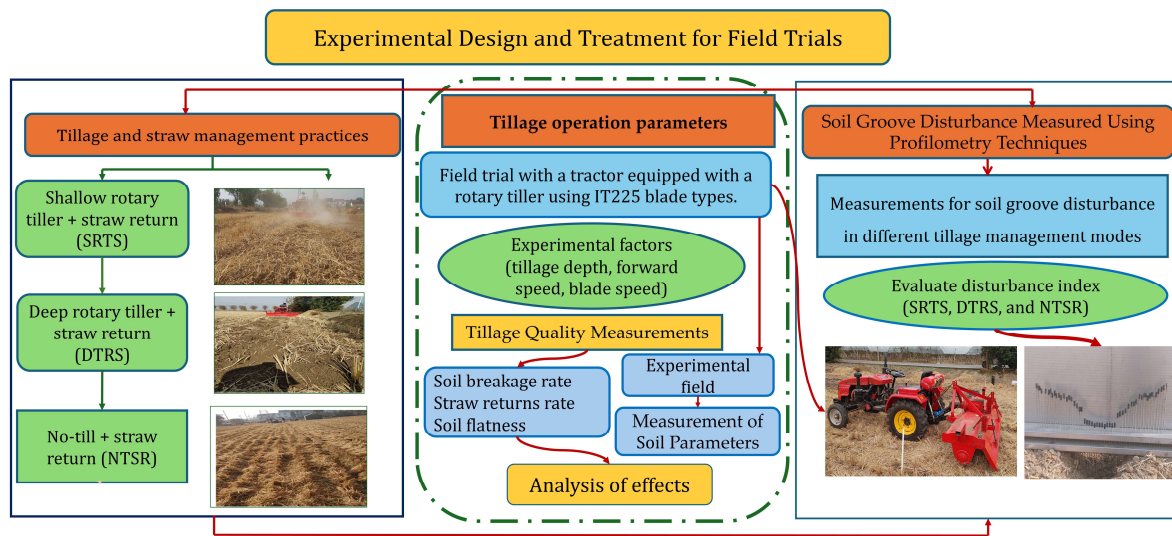

Figure 3. Flowchart of the experimental field layout and photographs of each tillage procedure employed in the present study.

2.2. Measurement of Soil Parameters

Soil mechanical factors, such as particle size distribution, cone index, bulk density, moisture content, pH, and nutrient levels (N, P, and K), are the primary parameters that define the nature of the interaction between soils and agricultural machines in terms of the soil's physicochemical characteristics. So, the chemical and physical features of the soil need to be quantified [28]. Studying the physical properties of the soil is crucial. The test method is broken down into broad categories when examining the characteristics of soil. Cone penetrometers are what we test with. The force necessary to crush a specific soil area yields the soil strength index (kPa) [29]. A gravimetric approach was used to determine the

moisture content in the paddy soil under the use of rotary tillers of 1GKN-180 paddy soil using the gravimeter method, and 1GKN-180 rotary tiller operation was also carried out.

2.3. Soil Groove Disturbance Measured Using Profilometry Techniques

Measurements were taken to assess soil groove disturbance in three tillage management modes: shallow rotary tiller + straw return (SRTS), deep rotary tiller + straw return (DTRS), and no-till + straw return (NTSR). We utilized a profilometer to create a 3D representation of the surface topography to identify the most severe disturbances occurring at the points where soil interacted with tools for performing tillage operations. The extent of disturbance changed with style, and the level of soil disturbance after the disturbance index evaluated cultivation. It can be put across as follows:

$$\text{SDI} = \frac{A}{D} \tag{1}$$

where A is the soil's mobilized area (cm^2), and D is the maximum groove depths (cm).

2.4. Tillage Operation Parameters

Tillage quality measurements included soil breaking rate, straw return rate, and surface roughness. After completing the rotary-mixed straws with soil operations, a 50-metre-long experimental field was chosen to measure and calculate quality parameters according to standards 1GKN-180 GB/T 5668-2017. Soil breakage rate, straw return rate, and soil flatness were evaluated as indicators. The following describes the methods for measuring and computing these indicators.

2.4.1. Soil Breaking Rate

The equation for soil broken rate has been defined as the percentage ratio of masses occupied by soil blocks with their greatest edges not exceeding four centimeters relative to all chains within the tillage horizon from a 500×500 (mm) sample location with a specified formula [27], as follows:

$$R_1 = \frac{m_a}{m_b} \times 100\% \tag{2}$$

where R_1 is the soil breakage rates, expressed in %; m_a is the mass, in kg, of the soil blocks in the total tillage layer whose longest side length is smaller than 4 cm; and m_b is the entire amount of soil in the tillage layer, in kg.

2.4.2. The Straw Return Rates

An essential metric for evaluating how straws move from the time they are cut until they decay is the return rate of straws. More efficient mixing and burying is suggested by a greater return rate [30,31]. We used a GB/T668 2017 "Rotary Tiller" method in analyzing the straw return rate, which was established by comparing the quantity of straw remaining on the ground level post-rotary tilling (operation of plowing). A 0.3 m $\times$ 0.3 m sample frame was then set on the ground. The sample frame (0.3 m $\times$ 0.3 m) was put on the ground. Straw above the ground surface was collected and weighed, while straw partially buried in the soil was cut with scissors against the ground surface.

The return rate of straw is then estimated based on the difference in the total weight of surface straw before and after rotary tillage using the equation below:

$$R_2 = \frac{P - P_1}{P} \times 100\% \tag{3}$$

where R_2 is a straw return rate; P is (kg) is the total weight of the straw before tilling; and P_1 (kg) is the total weight of the straw after plowing.

2.4.3. Soil Flatness

The precision of the surface profiling device, which can account for tractor motion, is demonstrated by [32]. The first step in determining the soil flatness is to average the height measurements along each of the ten routes—each with five measurement points—before and after the operation. The initial reference height is 21 mm, which is used to determine the average height before the procedure (h^{-after}), and measurements are divided by 40. To quantify soil flatness, calculate the average absolute divergence of the observed heights from the reference height after the procedure (h_{ref}). These computations help evaluate the impact of activities on soil flatness by providing a precise measure of change [33,34].

$$R_3 = \frac{1}{10 \times 5}\sum_{i=1}^{10}\sum_{j=1}^{n}|h_{ij}^{after}-h_{ref}| \tag{4}$$

where R_3 is a soil flatness, i represents the route number (1 to 10), and j represents the measurement point number (1 to 5) within that route.

2.4.4. Tillage Depth

The deep-loosened device tillage depth measuring system is of good significance in practice, popularization, and application value; it efficiently modifies tillage depth and secures state subsidies during the cultivating process [25]. The tillage depth was determined by putting a steel ruler into the soil and selecting a tillage depth where tillage depths were consistent. For tillage depth measurement, three points were measured at one-meter intervals within each row, and a total of 120 measurement points were collected across all rows [28]. The formulas that can be used to calculate cultivation depth includes n, the entire number of points of measure. This is a measure of plow depth, where h is the soil depth (in cm).

$$h = \frac{1}{n}\sum_{i=1}^{n}h_i \tag{5}$$

where h is the mean tillage depth (cm), h_i is the tillage depth at the i-th measurement point (cm), and n is the total number of measuring points.

2.4.5. Box–Behnken Design

Three factors are included in the BBD and RSM tools. One way to predict the optimal value of three factors is by using a second-order polynomial equation model [35–37]. Table 3 shows that the three-level and three-factorial Box–Behnken design of experiments required 17 runs of trials in total. The model is configured as follows:

$$\gamma = \beta_0+\sum\beta_iX_i+\sum\beta_{ij}X_i^2+\sum\sum\beta_{ij}X_iX_j \tag{6}$$

where γ is the expected response (phenol removal rate, %) utilized as a dependent variable, i = 1, 2, 3, and j = 1, 2, 3; β_0, β_i, and β_{ij} are the model regression coefficient parameters, and X_i is the input controlling coded variable and, furthermore, the natural variable of the operating system (X_j).

Table 3. Three factors and three levels of tillage operation parameter optimization.

Level	Forward Speed of Tractor Y_1 (km/h)	Rotation Speed of Blade Y_2 (rpm)	Depth of Field Operation Y_3 (cm)
−1	1.8	240	5
0	3.6	270	10
1	5.4	300	15

2.5. Test Factor

The primary purpose of the field experiment is to identify the optimal operating parameters of 1GKN-180 rotary tiller, as well as find out the roles of different components in incorporating straws and the quality of the soil. These variables include the blade revolution rate in rpm, the depth of field operations in cm, and the forward speed in km/h of the rotary tillage blade configuration. There are three levels to each component, and the following criteria were used to define them. The forward speed was controlled at three levels, 1.8, 3.6, and 5.4 (km/h), to provide sufficient soil disruption. According to the practical test specified for the rotary tiller in GB/T 5668-2017 Rotary Tiller, the rotary tiller blade roller was operated at three distinct rotational speeds—240, 270, and 300 rpm—to assess their impact on straw return rates. For covering the tillage operation, the tillage depth was manipulated through the tractor's three-point suspension and was set at 5, 10, and 15 cm. Quantitative assessment of the straw return rate was performed from the comparative analysis of straw quality on the ground level before and after the operation of rotary tillage. Thus, applying Design-Expert 13.0 software, they used the Box–Behnken approach in the development of the design of the experiment. The application of the Box–Behnken design enabled the identification of all the aspects of the chosen tillage practices that affect straw incorporation most effectively, as well as the interaction between them. Table 3 shows a list of the variables investigated in the study and the levels corresponding to the variables.

2.6. Data Analysis

The results from the experiment were statistically analyzed using Microsoft Excel's first experiment's one-way factorial analysis of variance (ANOVA). Treatment means that demonstrated statistical significance at the $p = 0.05$ probability level, as revealed by the F-test, were separated using the least significant difference (LSD. 0.05) test. The statistical data from experiment two were examined using Design Expert, a statistical model software product (13.0 version) from Stat Ease Inc., Minneapolis, MN, USA. The F-value shows how much of the mean square is attributable to regression from the mean square resulting from actual error. About soil breaking rate, straw return rate, and soil flatness, this software assesses the lack of fitness importance of both independent variables and the linear and cross-product impacts of dependencies.

3. Results and Discussion

3.1. The Effects of Soil Groove Disturbance Measured Using Profilometry Techniques After Tillage

The profilometry technique quantified soil disturbance by providing a three-dimensional representation of the soil surface following tillage. The deepest portion of the groove is indicated by its largest vertical distance from the groove bottom to the soil surface, both in the field and in Microsoft Excel, which is displayed in Table 4.

A p-value < 0.05 indicated significant variations in the averages of lateral and depth positions, affecting soil disturbance under different tillage management modes. Profilometry techniques contained graphical profiles and average readings, while the disturbance of DRTS mode was considerably the highest, SRTS mode was moderate, and NTSR mode did not disturb significantly. The layout of a profilometer used in identifying the depth and the horizontal position of the influenced soil area due to different tillage practices is illustrated in Figure 4a. In a profilometer, the vertical rods record the soil surface topography after tillage, which is important in identifying the displacement of the soil. The profile of the soil shown in Figure 4b was made by using the SRTS mode, which shows the soil depth after the tillage operation with consistency of variance as occurs depending on the position of the tiller in the lateral plane. In detail, Figure 4c gives the distribution of the NRSR of tillage methods about the effect of tillage depth distribution and lateral soil movement.

Based on Figure 4d, it is clear that the deep tillage system leads to a more enhanced and deeper soil championship than the other methods represented by the graph's depth.

Table 4. ANOVA: one-way factorial analysis of variance.

Groups	Count	Sum	Average	Variance	
Lateral position (cm) AV	27	365.3517	13.53154	68.43675	
Depth (cm) AV	27	201.6978	7.47029	31.30459	
Analysis of variance					
Source of Variation	SS	DF	MS	F	*p*-value
Among Groups	495.9739	1	495.9739	9.945202	0.002678 *
Within Groups	2593.275	52	49.87067		
Total	3089.249	53			

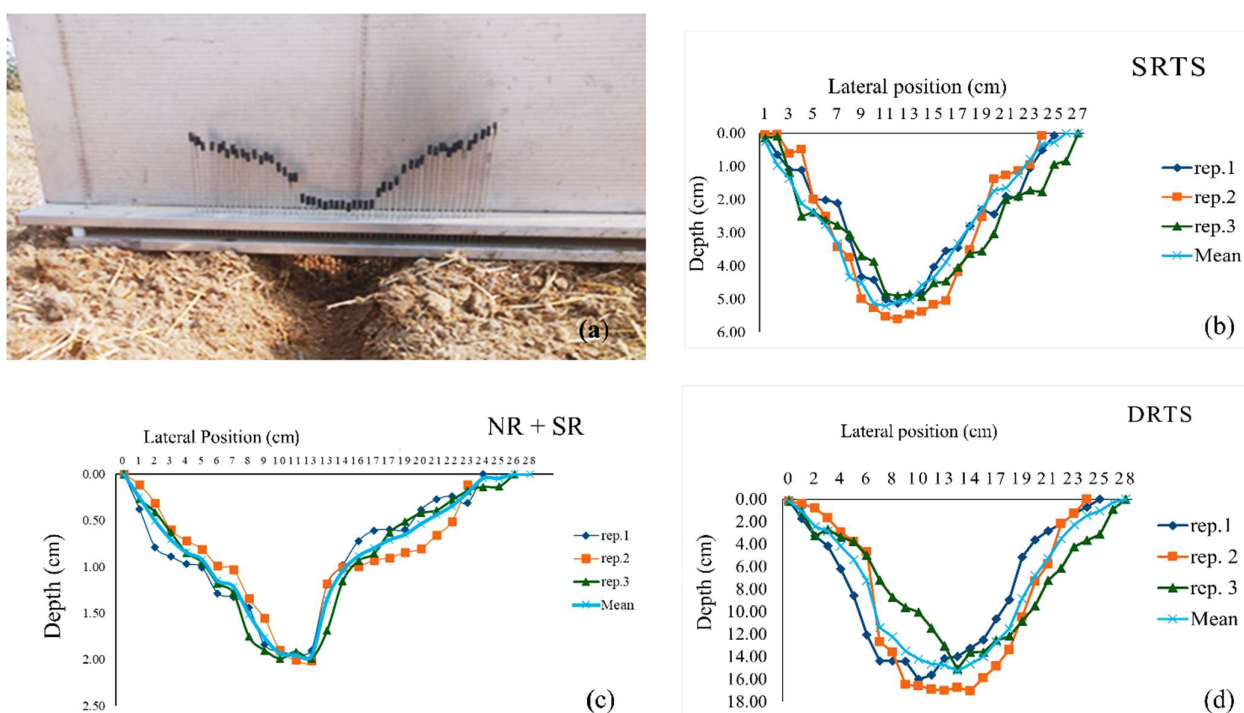Note: * shows significance ($p < 0.05$).

Figure 4. Profilometer of soil disturbance index: (**a**) Profilometer of sticks; (**b**) SRTS; (**c**) NTSR; (**d**) DRTS; a visual representation of the acquired profile and mean readings, respectively.

These graphical representations and average readings show how the tillage management modes affect the soil profile to a considerable extent. Thus, by assessing these profiles, it is possible to identify which tillage method is more efficient in causing the necessary impact on the soil, which is important for the optimization of agricultural work and the condition of the soil.

3.2. The Impact of Single Factors on Straw Return Rate

Figure 5 discusses an analysis of the effects of three factors (tillage depth, forward speed, and rotating speed) on straw return rate. The findings demonstrate that there is a correlation between forward speed and straw return rate at the rate of 3.06 km/h, which is depicted in Figure 5a. However, it has increased to 5.4 km/h, resulting in a small negative value, which indicates the optimal forward speed at which the maximum amount of straw can be returned. As the rotary blade speed increased from 240 rpm to 270 rpm, as shown in Figure 5b, it was observed that the straw return rate primarily increases when there is more

aggressive mixing of soil and residue. However, from a realistic perspective, it predicts that the returns start becoming smaller; hence, any increase beyond 300 rpm would not yield much. As the depth of tillage operations used for returning straw also rises, the straw return rate, presented in Figure 5c, also rises, up to 90%, and reaches 95% at a length of 10–15 cm. This increase is perhaps a result of increased root mass and the number of straw residues on the soil. Figure 5d demonstrates that higher speeds and deeper tillage increase the amount of straw incorporation. This also illustrates that the straw return rate corresponding to rotary blade speed rises at the shallow depths (0–5 cm), the moderate depths (5–10 cm), and the deeper levels (10–15 cm). Accordingly, the results derived from single-factor tests reveal that the depth of cultivation and rotary blade speeds significantly affect the straw return rate, and the deeper tillage and moderately high to high rotational speeds yielded better results. The combined effect of these factors implies that improving both parameters can improve straw burial, which is paramount for soil health and crop yields.
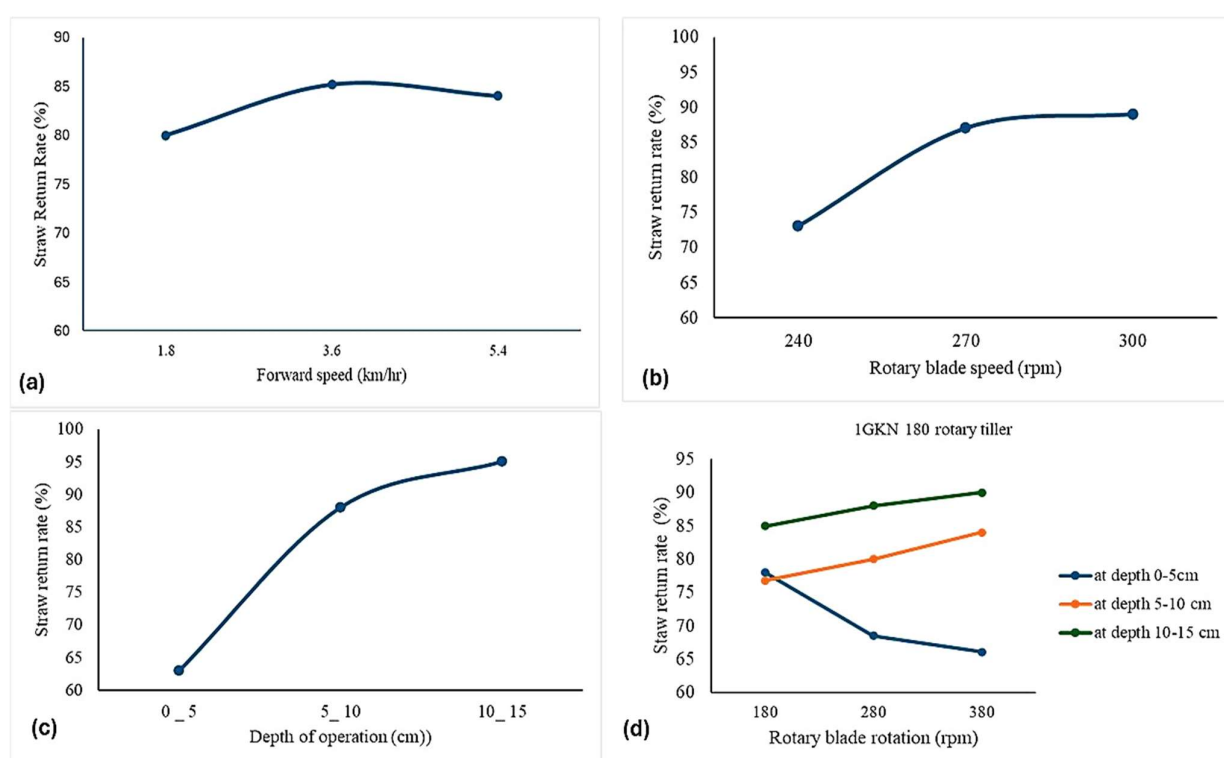

Figure 5. The impact of single factors on straw return rate: (**a**) forward speed vs. straw return rate; (**b**) rotary speed vs. straw return rate; (**c**) depth of operation against straw return rate; and (**d**) a combination of rotary blade rotation speeds and tillage depths vs. straw return rate.

3.3. Optimization of Operational Parameters Using Box–Behnken Design

3.3.1. Experimental Results

The parameter optimization test system for tillage operation parameters was designed using the three-factor, three-level Box–Behenken response surface trials. Table 5 displays the particular test plan as well as the test data results that were acquired.

The test results shown in Table 5 were analyzed using Design Expert 13.0, which included generating regression equations, ANOVA, creating response surface diagrams, analyzing influence factor interactions, and identifying the optimal parameter combination.

Table 5. Test scheme and results of optimization of tillage parameters.

	Independent Variables (Factors)			Response Value		
Runs	Forward Speed $Y_1(\frac{km}{h})$	Rotary Tillage Blade Y_2 (rpm)	Depth of Soil Layers, Y_3 cm	Soil Breaking Rate R_1 (%)	Straw Return Rate (%) R_2 (%)	Soil Flatness R_3 (mm)
1	1.8	270	15	92	82.7	13
2	3.6	270	10	86.7	77.8	17
3	3.6	270	10	87	78	17.5
4	3.6	240	5	78.2	65.5	20.5
5	5.4	270	5	79.5	67.5	19.5
6	3.6	270	10	87.4	77.5	17
7	1.8	300	10	88	82.3	14
8	5.4	300	10	89	83.8	16
9	3.6	300	15	96.7	84.7	10
10	3.6	300	5	83.1	73.9	16.5
11	3.6	270	10	86.8	77.8	17.5
12	5.4	270	15	92.2	80.4	13
13	1.8	240	10	80	79.9	21
14	3.6	270	10	86.1	77	17.5
15	5.4	240	10	84.2	76	17.5
16	3.6	240	15	93.5	82.8	15.5
17	1.8	270	5	73.8	67.6	20

3.3.2. Regression Equation Construction

The regression equation that established the relationship between the test indicators and the test components was developed using multiple regression analyses of the collected data. Such an equation is expressed as Equation (7). The attainment above represents the outstanding predictivity achievable on a real value versus predicted value relationship regarding optimized tillage operation parameters. The strength of this model may place it in the position of being quite a resource tool for agricultural optimization due to its ability to forecast such parameters as critical measures with great accuracy—the rate of soil breakage, the returning rate of straw, and soil flatness. A further indicator is that such extrapolations fall within well-defined control limits for a wide range of parameter settings, showing the stability and dependability of the optimization process.

Ultimately, both the field measured real-world quantities and their predictions in relation to optimized tillage operations are related by Model Equation (7). This fact underscores the significant practical value of the model in a multitude of agronomic applications, proving its efficiency in enabling farm practice improvements and increasing crop yields through enhanced soil management techniques.

$$
\begin{cases}
R_1 = 89.31 + 11.85Y_1 - 0.431Y_2 + 2.750Y_3 - 0.0148Y_1Y_2 - 0.1528Y_1Y_3 - \\
\qquad 0.0038Y_2Y_3 - 0.7716Y_1^2 + 0.0011Y_2^2 + 0.030Y_3^2 \\
R_2 = 227.03 - 7.256Y_1 - 1.413Y_2 + 7.286Y_3 + 0.0250Y_1Y_2 - 0.0611Y_1Y_3 + \\
\qquad 0.0108Y_2Y_3 + 0.1088Y_1^2 + 0.0028Y_2^2 - 0.1369Y_3^2 \\
R_3 = 21.64 - 7.792\,Y_1 + 0.136Y_2 + 0.970Y_3 + 0.0255Y_1Y_2 + 0.0139Y_1Y_3 - \\
\qquad 0.0025Y_2Y_3 + 0.0887Y_1^2 - 0.0005Y_2^2 - 0.0485\,Y_3^2
\end{cases} \tag{7}
$$

where R_1 is soil breakage rate (%); R_2 is straw returning rate (mm); R_3 is soil flatness, mm; Y_1 is forward speed (km/h); Y_2 represents the blade's rotation speed (rpm); and Y_3 is the soil depth (cm).

The comparison of real and anticipated values for optimal tillage operation parameters demonstrates outstanding predictive ability. The model can accurately predict soil breaking rate, straw return rate, and soil flatness, making it an important tool for agricultural optimization

3.3.3. The Analysis of the Breakage Rate Model

The primary and secondary order of the effect of numerous factors on soil breaking rate, as well as the model's appropriate accuracy, were determined by analyzing soil breakage rate data with ternary quadratic regression and variance analysis.

Table 6 shows a substantial difference across regression models (F = 82.8, $p < 0.0001$). The adjusted values are 0.9787 and 0.9902. Furthermore, the not-fit test yielded F = 1.48, $p > 0.1$, indicating that the result is not significant. Table 6 reveals that the model had the biggest effect on the soil breaking rate index's key components. Y_3 significantly affected soil cracking rates ($p < 0.05$). There are three primary and secondary factors correlated with the soil breaking rate, instructed as $Y_3 > Y_2 > Y_1$.

Table 6. Variance analysis of the soil breakdown rate equation for regression.

The source	Sum of Squares	Level of Freedom	The Mean Square	F-Value	*p*-Value
Model	1251.88	9	139.1	82.8	<0.0001 *
Y_1-Forward speed	17.11	1	17.11	10.19	0.0152
Y_2-Blade speed	57.78	1	57.78	34.4	0.0006
Y_3-Depth of soil	1053.41	1	1053.41	627.05	<0.0001 *
$Y_1 Y_2$	1.1	1	1.1	0.6563	0.4445
$Y_1 Y_3$	20.25	1	20.25	12.05	0.0104
$Y_2 Y_3$	1.21	1	1.21	0.7203	0.4241
Y_1^2	23.1	1	23.1	13.75	0.0076
Y_2^2	0.1044	1	0.1044	0.0622	0.8103
Y_3^2	73.13	1	73.13	43.53	0.0003 *
Residual	11.76	7	1.68		
Lack of Fit	6.19	3	2.06	1.48	0.3471
Pure Error	5.57	4	1.39		
Cor Total	1263.64	16			
R^2	0.9992				
Adjustment of R^2	0.9982				

Note: * indicates significance ($p < 0.05$).

We conducted a response surface analysis based on the regression model to investigate the interaction effects of key influencing factors on the evaluation indicator R_1. The quadratic polynomial regression equation was reduced by fixing one factor at its zero level to isolate and analyze the interaction effects of the other two factors, excluding insignificant terms. Effects Y_1 and Y_2 on R_1 are demonstrated in Figure 6b, where the response surface demonstrates the interaction of a non-linear nature with an optimal range for greater soil breaking rates. Figure 6c also covers the interaction of factors Y_1 and Y_3 on R_1 as a whole, indicating that deeper depth into the soil and a moderate forward speed gives good performance in soil breaking performance. Finally, Figure 6d implies the interaction between the other two, Y_2 and Y_3, and shows that high blade speeds and lower soil depths significantly influence the soil breaking rate. These response surfaces highlight that fine-tuning between these parameters has high stakes for efficient soil breaking.

3.3.4. The Analysis of the Straw Return Rate Model

Variance analysis and ternary quadratic regression were employed to evaluate the appropriate accuracy of the given model and examine the first- and second-order effects of various parameters on the straw return rate.

Table 7 shows adjusted values of 0.9902 and 0.9787, with a significant difference across regression models (F = 1025.39, $p < 0.0001$). Furthermore, the not-fit test yielded an insignificant result (F = 0.8153, $p > 0.1$). The model with the largest effect on the straw return rate index in the critical item is shown in Table 7. This had a significant influence on the straw return rate ($p < 0.05$). The straw return rate was correlated with three major and secondary attributes: $Y_3 > Y_2 > Y_1$.
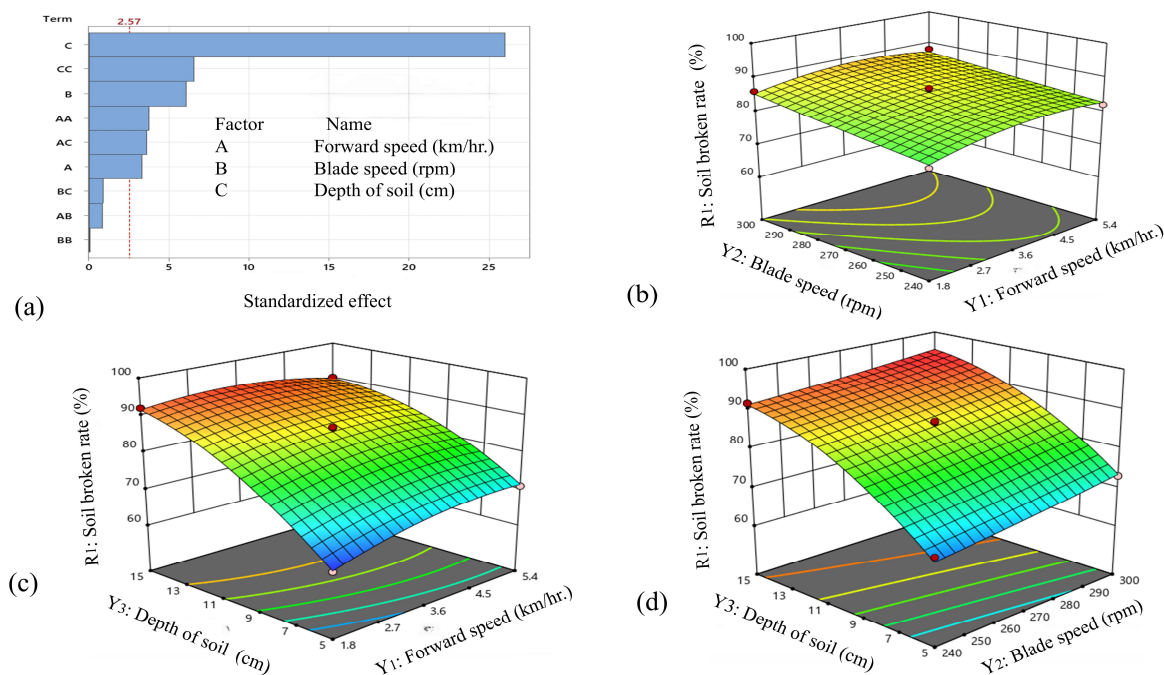
Figure 6. Displays the response of the surface to factors affecting soil breaking rate: (**a**) The Pareto chart depicts the standardized effects of different variables on soil breaking; (**b**) This plot shows how the soil breaking rate changes with variations in forward speed and blade speed; (**c**) This plot depicts the combined effect of forward speed and soil depth on straw return rate; and (**d**) This plot shows the interaction between blade speed and soil depth.

Table 7. Variance analysis of the straw returning rate regression equation.

The Source	Sum of Squares	Level of Freedom	Mean Square	F-Value	*p*-Value
Model	1572.15	9	174.68	1025.39	<0.0001 *
Y_1-Forward speed	1.36	1	1.36	7.99	0.0255
Y_2-Blade speed	66.13	1	66.13	388.16	<0.0001 *
Y_3-Depth of soil	1178.55	1	1178.55	6918.12	<0.0001 *
$Y_1 Y_2$	3.8	1	3.8	22.32	0.0021
$Y_1 Y_3$	1.21	1	1.21	7.1	0.0322
$Y_2 Y_3$	14.06	1	14.06	82.55	<0.0001 *
Y_1^2	0.3789	1	0.3789	2.22	0.1795
Y_2^2	20.84	1	20.84	122.36	<0.0001 *
Y_3^2	293.57	1	293.57	1723.25	<0.0001 *
Residual	1.19	7	0.1704		
Lack of Fit	0.4525	3	0.1508	0.8153	0.5487
Pure Error	0.74	4	0.185		
Cor Total	1573.34	16			
R^2	0.992				
Adjustment of R^2	0.998				

Note: * shows significance (*p* < 0.05).

Response surface analysis was used to investigate the interaction effects of influencing factors on straw return rate, setting one factor to zero and excluding non-significant terms. The Pareto chart in the upper left indicates that soil depth has the largest impact on the straw return rate, soil breakage rate, and short-period forward speed, in which the overlay of medium blade speed with an optimal forward speed provided the highest return was shown in Figure 7b, which shows the practice of straw return as the effects on Y_1 and Y_3. Figure 7c chooses lower soil depths with the not-too-high forward speed as the optimal straw return. Figure 7d elucidates the mutual actions of Y_3 and Y_2, stating that higher soil speeds combined with moderate depth enhance straw return efficiency. They are

highlighting the essential requirement of accurate parameter optimization to have good straw return performance.
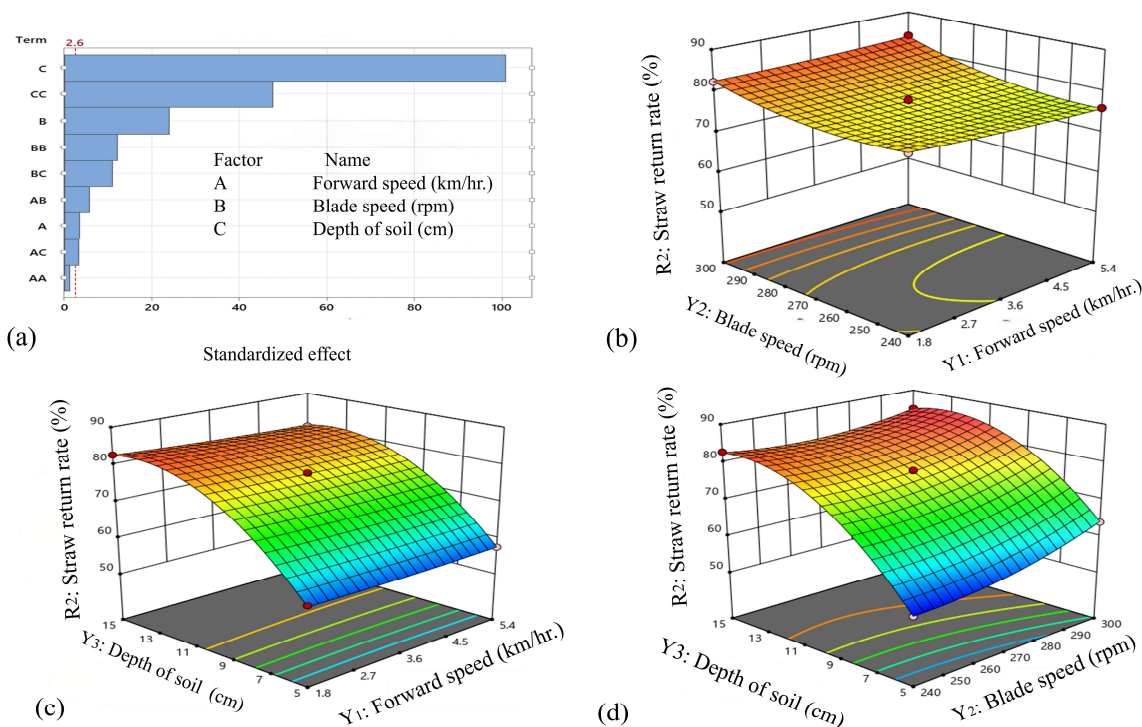

Figure 7. Displays the tillage operational parameter effects on straw return: (**a**) The Pareto chart represents the standardized effects of various factors on the straw return rate; (**b**) This plot depicts how the straw return rate changes when forward speed and blade speed varies; (**c**) This plot depicts the combined influence of forward speed and soil depth on straw return rate; and (**d**) This plot depicts the inter-action between blade speed and soil depth.

3.3.5. Analysis of Soil Flatness Model

To ascertain the proper accuracy of the model and the primary and secondary order of the influence of various factors on soil flatness, variance analysis, and ternary quadratic regression analysis were used for the soil flatness records. Table 8 demonstrates that the corrected values are 0.998 and 0.996, respectively. Additionally, the model importance test yields a significant difference between the regression models ($F = 507.42$, $p < 0.0001$). Additionally, $F = 0.0134$, $p > 0.1$ in the not-fit test indicates insignificance. Table 8 demonstrates that the model had the biggest impact on the main item's soil flatness index. Y_2, Y_3, Y_2, and Y_3 had a statistically significant ($p < 0.05$) impact on soil flatness. Three characteristics had a major and secondary relation to soil flatness: $Y_2 > Y_3 > Y_1$.

The response surface analysis was conducted to study the influence of important factors in soil flatness focusing on the significant interface between forward speed Y_1, Y_2, and Y_3 in the response. Y_3 is the most influential factor of soil flatness in Figure 8a in terms of standardized effects of agricultural variables, Y_3, followed by Y_2 and Y_1. Figure 8b shows the interaction between Y_1 and Y_2; the lower the two variables combined, the smoother the tillage surface. Figure 8c presents the superposition of Y_1 and Y_3, where it showed that a lower forward speed along deeper soil depth was associated with higher soil flatness. Lastly, Figure 8d illustrates the interaction between Y_3 and Y_2, and data tell higher blade speeds and deeper soil depths at the very best found in level challenges for soil flattening performance. The results highlight the necessity of fine-tuning these factors to improve soil flattening outcomes.

Table 8. Variance analysis of the soil flatness regression equation.

The Source	Sum of Squares	Level of Freedom	Mean Square	F-Value	*p*-Value
Model	492.89	9	54.77	507.42	<0.0001 *
Y_1-Forward speed	0.0013	1	0.0013	0.0116	0.9173
Y_2-Blade speed	42.32	1	42.32	392.11	<0.0001 *
Y_3-Depth of soil	24.15	1	24.15	223.77	<0.0001 *
$Y_1 Y_2$	3.06	1	3.06	28.38	0.0011
$Y_1 Y_3$	0.64	1	0.64	5.93	0.0451
$Y_2 Y_3$	54.02	1	54.02	500.54	<0.0001 *
Y_1^2	15.04	1	15.04	139.36	<0.0001 *
Y_2^2	4.96	1	4.96	45.93	0.0003
Y_3^2	344.09	1	344.09	3188.14	<0.0001 *
Residual	0.7555	7	0.1079		
Lack of Fit	0.0075	3	0.0025	0.0134	0.9975
Pure Error	0.748	4	0.187		
Cor Total	493.64	16			
R^2	0.998				
Adjustment of R^2	0.996				

Note: * shows significance ($p < 0.05$).
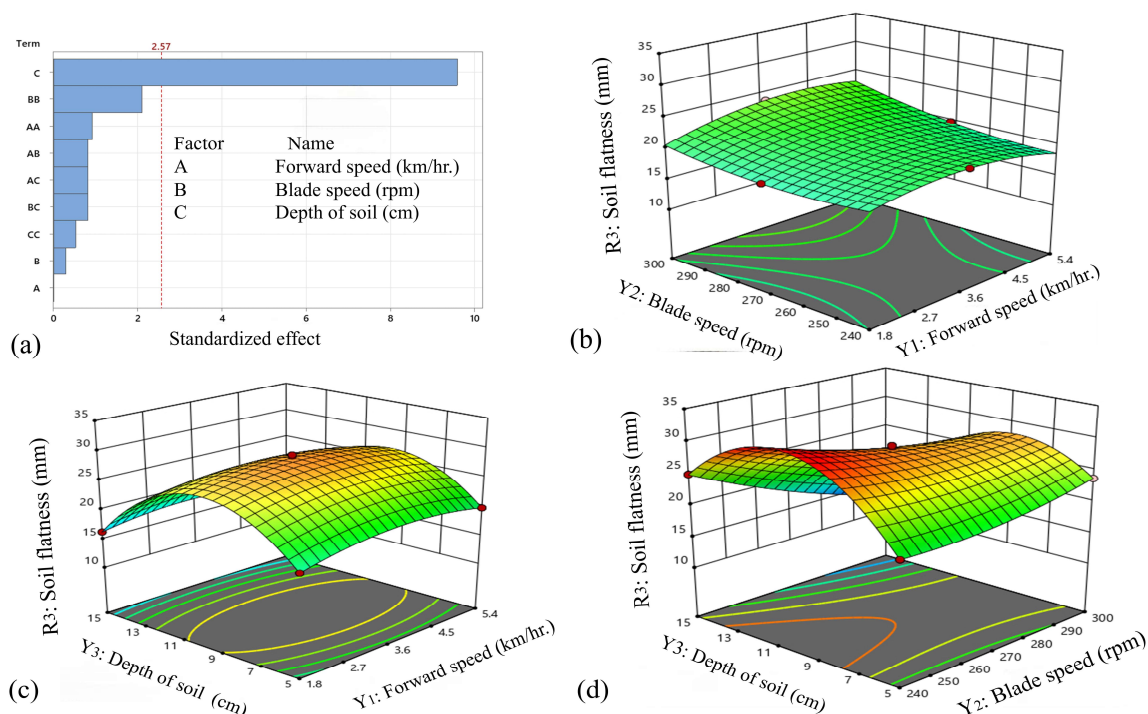
Figure 8. Shows how tillage operational parameters affect soil flatness: (**a**) The Pareto chart depicts the standardized effects of different factors on soil flatness. (**b**) This plot demonstrates how soil flatness varies with changes in forward speed and blade speed. (**c**) This plot shows how forward speed and soil depth work together to affect the straw return rate. (**d**) This plot shows how blade speed and depth of soil interact.

3.3.6. Desirability

The objectives of the experiment were thus to determine the optimal tillage depth, the blade rotational speed, and the forward speed to incorporate crop residues into the soil by using a TG-500 tractor and a Qingxuan 1GKN-180 rotary tiller. It was also observed that low forward speeds and high blade speeds were desirable for the generation of maximum efficiency, as seen from the desirability graphs. Through the response surface plots, it is observed that low forward speed, large blade speed, and small tillage depth gave the highest value of straw incorporation. Again, the desirability graphs indicate an illustration of how the various operational parameters affect the efficiency of smooth incorporation in

the end. From the view of Figure 9a, it can be seen that low forward speeds and high blade speeds lead to the highest value of desirability, which indicates the best straw incorporation. Figure 9b shows that acceptable corrections are achieved at low forward speeds and at small tillage depths, which are correspondingly lower than the desired ability for a tool at high forward speed and deep tillage. These conclusions are further supported by Figure 9c, which depicts that desirability decreases with increasing depth of the soil and is at its maximum at high blade speeds and shallow depths of the soil.

(a)   (b)   (c)
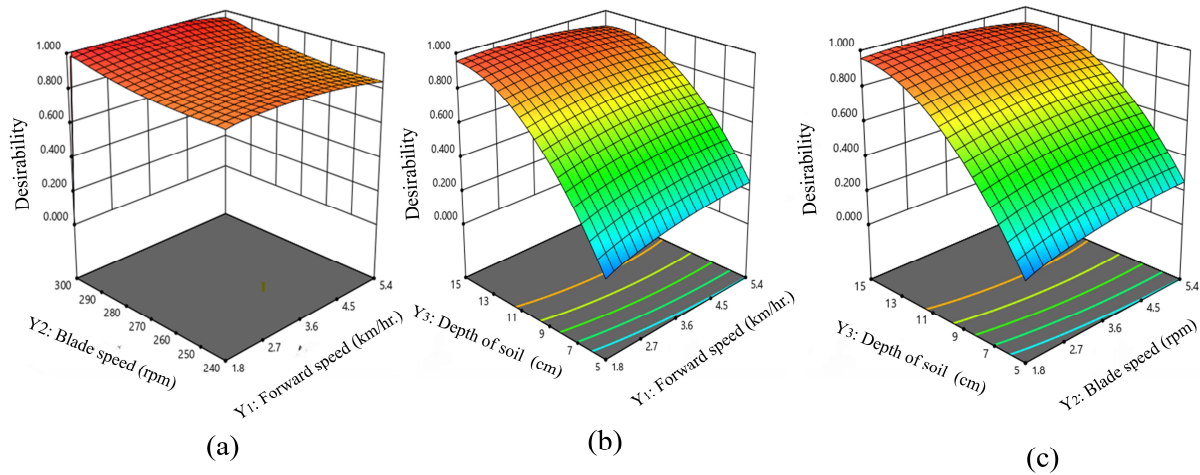
Figure 9. The desirability graph: (**a**) shows that low forward speeds and high blade speeds result in the highest desirability; (**b**) indicates that desirability decreases as forward speed and soil depth increase, with low forward speed and shallow depth yielding the best results; and (**c**) shows that as soil depth increases, desirability decreases from its peak at high blade speeds and shallow soil depths.

3.4. Optimizing Parameters and Validating the Model

The second-sequence polynomial model was used to increase quality in straw incorporation by adjusting the tillage operation parameters in a Qingxuan 1GKN-180 rotary tiller to enhance overall performance regarding the maximization of the rate of straw return, maximum soil breaking, and rate of in-range soil flatness. Improving the amount of straw added to the rice-wheat (RW) rotation field is the main goal of this optimization. The regression model was solved using the Design-Expert 13.0 programmers optimization module and the following intended results were formulated mathematically.

$$\begin{cases} \max R_1(Y_1, Y_2, Y_3) \\ \max R_2(Y_1, Y_2, Y_3) \\ \text{in range } R_3(Y_1, Y_2 Y_3) \\ \text{s.t.} \begin{cases} 1.8\frac{km}{hr} \leq Y_1 \leq 5.4\frac{km}{hr} \\ 240 \text{ rpm} \leq Y_2 \leq 300 \text{ rpm} \\ 5 \text{ cm } \leq Y_3 \leq 15 \text{ cm} \end{cases} \end{cases} \tag{8}$$

The optimal set of design solutions was developed using an optimization method, with a forward speed of 3.23 km/h. The operational depth of the rotary tillage blade rollers was 14.23 cm, with a rotating speed of 297.6 rpm. After adjusting the tillage operation parameters to approach the ideal solution, three further trials were undertaken to check the precision of the optimized parameters. Specifically, 3.23 km/h was the maximum forward speed limit used during a rotary tillage test for straw incorporation. The rotary blade ran at 14.23 cm of depth and 297.6 rpm. The verification test results showed that the average soil breaking rate was 94.76%, the straw covering rate was 84.97%, and the soil flatness was 16.36 mm under the optimal operating settings that the software determined. This

model was deemed credible when the relative error between the test value and the model optimization value was 5%. Regression model errors of 5.57%, 0.74%, and 0.748% show the precision of the tested model of optimization of parameters. A mathematical model that links tillage operation parameters with straw management is very important for the optimization of tillage parameters and field data in tillage operation parameters.

3.5. Discussion

The results of this study contribute to the enhancement of tillage operation characteristics that enhance straw management in rice-wheat cropped systems. The profilometry techniques with sticks provided adequate details of the surface features of the soil after tilling; therefore, adequate assessment of the degree of soil disturbance could be conducted. The corresponding graphical illustrations also indicated that the DRTS mode was most disturbing, the SRTS mode was moderately disturbing, and the NTSR mode was least disturbing. The setup determined the depth and the lateral distance that was disturbed by the implements, which showed how the various tillage implements affected the level of soil disturbance. Deep tillage had the most significant amount of disruption to the soil. It is essential to comprehend these profiles to improve the productivity of farming, as well as improve the state of the soil.

Utilizing the BBD and RSM, we identified and validated the optimal settings for three critical factors: given by forward speed, blade speed, and operating depth. The optimum parameters include a forward rate of 3.23 km/h, a rotary tillage blade speed of 297.6 rpm, and an operating depth of 14.23 cm—which results in significant improvements in tillage quality. Validation tests showed a high soil breaking rate of 94.76%, an impressive straw return rate of 84.97%, and an in-range soil flatness deviation of 16.36 mm. This shows that the optimized results agree well with the actual outcomes, enjoying a relative error of less than 5%,;this ascertains the reliability of the developed optimization model. Increased values of some parameters in the rice-wheat system incorporation of straw lead to enhanced soil health and environmentally friendly systems. The paper under consideration equally focuses on the need to incorporate straw and tillage operation parameters to support the health of the rice-wheat system and increase crop yield. Based on this study, it is revealed that there is evidence of incorporating straw if the Qingxuan 1GKN-180 rotary tiller is used with some operational changes. The investigators also confirmed this by applying the mathematical model. The average relative errors in the study were below 0.05, implying the generalization of the study. However, more confirmation is required, although the paper outlined a systematic way of improving the performance of tillage tools.

4. Conclusions

The present study used a stick profilometer, which is one of the more convenient devices for studying the soil profile. It is imperative to note that tillage practices disrupt the soil to various extents, thus proving to have various impacts on the profiles of the soil. Thus, the Box–Benhken design, with the help of RSM, was employed to find conditions for the maximum values of soil breaking rate, soil flatness, and good straw return rate. By applying regression modeling and analysis of variance (ANOVA), it explained that the important components and their interaction were found significant for the indicated tillage optimization framework. From the trials performed on the Qingxuan 1GKN-180 rotary tiller, it was observed that controlling the operational parameters enhanced excellent improvements in the quality of tillage. A rigorous maximum optimization algorithm determined the following optimal parameters: 3.23 km/h of forward speed, 297.6 min^{-1} of rotary blade speed, and 14.23 cm of operating depth. The mean tested value of the soil breaking rate was 94.76%, straw returns were 84.97%, and the deviation of the soil surface

was 16.36 mm on average. So, it can be concluded that the model dependency was highly significant because the error never exceeded 5% relative to the model predictions. It plays a major role as an operational state factor when adjusting the parameters of plowing, since this influences the particular performances of plowing during field operations.

Thus, future research work should be directed toward the assessment of the sustainable impact of diversified tillage practices in different regions on indices of soil health so that straw management in rice-wheat areas could be determined in a manner that accelerates nutrient mobilization and minimizes the emission of greenhouse gases at the same time.

References

1. Akwakwa, G.H.; Xiaoyan, W. Impact of Rice–Wheat Straw Incorporation and Varying Nitrogen Fertilizer Rates on Soil Physico-chemical Properties and Wheat Grain Yield. *Agronomy* **2023**, *13*, 2363. [CrossRef]
2. Lacroix, C.; Vandenberghe, C.; Monty, A.; Dumont, B. Effect of long-term tillage and residue management on weed flora and its impact on winter wheat development. *Agric. Ecosyst. Environ.* **2024**, *366*, 108937. [CrossRef]
3. Aikins, K.A.; Barr, J.B.; Antille, D.L.; Ucgul, M.; Jensen, T.A.; Desbiolles, J.M. Analysis of the effect of bent leg opener geometry on performance in cohesive soil using the discrete element method. *Biosyst. Eng.* **2021**, *209*, 106–124. [CrossRef]
4. Bhatt, R.; Singh, P.; Hossain, A.; Timsina, J. Rice–wheat system in the northwest Indo-Gangetic plains of South Asia: Issues and technological interventions for increasing productivity and sustainability. *Paddy Water Environ.* **2021**, *19*, 345–365. [CrossRef]
5. Mu, G.; Wang, W.; Zhang, T.; Hu, L.; Zheng, W.; Zhang, W. Design and Experiment with a Double-Roller Sweet Potato Vine Harvester. *Agriculture* **2022**, *12*, 1559. [CrossRef]
6. Conte, O.; Levien, R.; Debiasi, H.; Stürmer, S.L.; Mazurana, M.; Müller, J. Soil disturbance index as an indicator of seed drill efficiency in no-tillage agrosystems. *Soil Tillage Res.* **2011**, *114*, 37–42. [CrossRef]
7. Xu, G.; Xie, Y.; Liang, L.; Ding, Q.; Xie, H.; Wang, J. Straw-Soil-Rotary Blade Interaction: Interactive Effects of Multiple Operation Parameters on the Straw Movement. *Agronomy* **2022**, *12*, 847. [CrossRef]
8. Fang, H.; Zhang, Q.; Chandio, F.A.; Guo, J.; Sattar, A.; Arslan, C.; Ji, C. Effect of straw length and rotavator kinematic parameter on soil and straw movement by a rotary blade. *Eng. Agric. Environ. Food* **2016**, *9*, 235–241. [CrossRef]
9. Gupta, R.K.; Sraw, P.K.; Kang, J.S.; Kaur, J.; Sharma, V.; Pathania, N.; Kalia, A.; Al-Ansari, N.; Alataway, A.; Dewidar, A.Z.; et al. Interactive effects of long-term management of crop residue and phosphorus fertilization on wheat productivity and soil health in the rice-wheat. *Sci. Rep.* **2024**, *14*, 1399. [CrossRef]
10. Tahmasebi, M.; Gohari, M.; Sharifi Malvajerdi, A.; Hedayatipour, A. Development and Field Evaluation of a Variable-Depth Tillage Tool Based on a Horizontal Pneumatic Sensor Measurement. *J. Agric. Mach.* **2023**, *13*, 85. [CrossRef]
11. Nawaz, A.; Farooq, M.; Nadeem, F.; Siddique, K.H.; Lal, R. Rice-wheat cropping systems in South Asia: Issues, options and opportunities. *Crop Pasture Sci.* **2019**, *70*, 395–427. [CrossRef]
12. Wu, F.; Xu, H.; Gu, F.; Chen, Y.; Shi, L.; Hu, Z. Improvement of straw transport device for straw-smashing back-throwing type multi-function no-tillage planter. *Nongye Gongcheng Xuebao/Trans. Chin. Soc. Agric. Eng.* **2017**, *33*, 18–26. [CrossRef]
13. Huang, J.; Nie, T.; Li, T.; Chen, P.; Zhang, Z.; Zhu, S.; Sun, Z.; E, L. Effects of Straw Incorporation Years and Water-Saving Irrigation on Greenhouse Gas Emissions from Paddy Fields in Cold Region of Northeast China. *Agriculture* **2022**, *12*, 1878. [CrossRef]
14. Song, K.; Yang, J.; Xue, Y.; Lv, W.; Zheng, X.; Pan, J. Influence of tillage practices and straw incorporation on soil aggregates, organic carbon, and crop yields in a rice-wheat rotation system. *Sci. Rep.* **2016**, *6*, 36602. [CrossRef]

15. Sarkar, S.; Skalicky, M.; Hossain, A.; Brestic, M.; Saha, S.; Garai, S.; Ray, K.; Brahmachari, K. Management of crop residues for improving input use efficiency and agricultural sustainability. *Sustainability* **2020**, *12*, 9808. [CrossRef]

16. Korav, S.; Yadav, D.B.; Yadav, A.; Rajanna, G.A.; Parshad, J.; Tallapragada, S.; Elansary, H.O.; Mahmoud, E.A. Rice residue management alternatives in rice-wheat cropping system: Impact on wheat productivity, soil organic carbon, water, and microbial dynamics. *Sci. Rep.* **2024**, *14*, 1822. [CrossRef]

17. Memon, M.S.; Guo, J.; Tagar, A.A.; Perveen, N.; Ji, C.; Memon, S.A.; Memon, N. The effects of tillage and straw incorporation on soil organic carbon status, rice crop productivity, and sustainability in the rice-wheat cropping system of Eastern China. *Sustainability* **2018**, *10*, 961. [CrossRef]

18. Li, Y.E.; Shi, S.; Waqas, M.A.; Zhou, X.; Li, J.; Wan, Y.; Qin, X.; Gao, Q.; Liu, S.; Wilkes, A. Long-term (≥20 years) application of fertilizers and straw return enhances soil carbon storage: A meta-analysis. *Mitig. Adapt. Strateg. Glob. Chang.* **2018**, *23*, 603–619. [CrossRef]

19. Feiziene, D.; Feiza, V.; Karklins, A.; Versuliene, A.; Janusauskaite, D.; Antanaitis, S. After-effects of long-term tillage and residue management on topsoil state in Boreal conditions. *Eur. J. Agron.* **2018**, *94*, 12–24. [CrossRef]

20. Wang, Y.; Qin, M.; Zhan, M.; Liu, T.; Yuan, J. Straw return-enhanced soil carbon and nitrogen fractions and nitrogen use efficiency in a maize-rice rotation system. *Exp. Agric.* **2024**, *60*, e5. [CrossRef]

21. Guo, R.; Li, G.; Pan, M.; Zheng, X.; Wang, Z.; He, G. Effects of Long-Term Straw Return and Nitrogen Application Rate on Organic Carbon Storage, Components and Aggregates in Cultivated Layers. *Sci. Agric. Sin.* **2023**, *56*, 4035–4048. [CrossRef]

22. Agarry, S.E.; Ogunleye, O.O. Box-Behnken design application to study enhanced bioremediation of soil artificially contaminated with spent engine oil using biostimulation strategy. *Int. J. Energy Environ. Eng.* **2012**, *3*, 31. [CrossRef]

23. Zhang, X.; Zhang, L.; Hu, X.; Wang, H.; Shi, X.; Ma, X. Simulation of Soil Cutting and Power Consumption Optimization of a Typical Rotary Tillage Soil Blade. *Appl. Sci.* **2022**, *12*, 8177. [CrossRef]

24. Zhang, J.; Xia, M.; Chen, W.; Yuan, D.; Wu, C.; Zhu, J. Simulation Analysis and Experiments for Blade-Soil-Straw Interaction under Deep Ploughing Based on the Discrete Element Method. *Agriculture* **2023**, *13*, 136. [CrossRef]

25. Ding, R. Study on measuring system of tillage depth of deep loosening machine. *J. Comput. Methods Sci. Eng.* **2017**, *17*, 473–480. [CrossRef]

26. Zhu, D.; Shi, M.; Yu, C.; Yu, Z.; Kuang, F.; Xiong, W.; Xue, K. Tool-straw-paddy soil coupling model of mechanical rotary-tillage process based on DEM-FEM. *Comput. Electron. Agric.* **2023**, *215*, 108410. [CrossRef]

27. Zhang, S.; Jia, X.; Dong, J.; Wang, X.; Zhao, H.; Chen, X.; Zhang, Z.; Huang, Y.; Shi, J. Optimization of operating angles of disc colters for maize residue management using discrete element method. *Comput. Electron. Agric.* **2024**, *218*, 108691. [CrossRef]

28. Kim, Y.S.; Kim, T.J.; Kim, Y.J.; Lee, S.D.; Park, S.U.; Kim, W.S. Development of a real-time tillage depth measurement system for agricultural tractors: Application to the effect analysis of tillage depth on draft force during plow tillage. *Sensors* **2020**, *20*, 912. [CrossRef]

29. Latvala, J.; Luomala, H.; Kolisoja, P. Determining soil moisture content and material properties with dynamic cone penetrometer. *Balt. J. Road Bridge Eng.* **2020**, *15*, 136–159. [CrossRef]

30. Tang, H.; Wang, D.; Zhao, J.; Xu, C.; Wang, J. Mode and experiments of a straw ditch-burying returning and maturing in a cold region of Northeast China. *Eur. J. Agron.* **2023**, *151*, 127006. [CrossRef]

31. Zhao, H.; Wu, L.; Zhu, S.; Sun, H.; Xu, C.; Fu, J.; Ning, T. Sensitivities of Physical and Chemical Attributes of Soil Quality to Different Tillage Management. *Agronomy* **2022**, *12*, 1153. [CrossRef]

32. Ehrhardt, A.; Deumlich, D.; Gerke, H.H. Soil Surface Micro-Topography by Structure-from-Motion Photogrammetry for Monitoring Density and Erosion Dynamics. *Front. Environ. Sci.* **2022**, *9*, 737702. [CrossRef]

33. Li, L.; Nearing, M.A.; Nichols, M.H.; Polyakov, V.O.; Guertin, D.P.; Cavanaugh, M.L. The effects of DEM interpolation on quantifying soil surface roughness using terrestrial LiDAR. *Soil. Tillage Res.* **2020**, *198*, 104520. [CrossRef]

34. Leanza, A.; Matranga, G.; Biddoccu, M.; Cavallo, E.; Milella, A.; Reina, G. Novel Measurements and Features for the Characterization of Soil Surface Roughness. *IEEE Access* **2022**, *10*, 131735–131746. [CrossRef]

35. Nursid, M.; Permatasari, A.; Syafitri, U.D.; Batubara, I. Application of Box-Behnken Design for the Extraction of Padina australis. *Molekul* **2022**, *17*, 270–280. [CrossRef]

36. Ferreira, S.C.; Bruns, R.E.; Ferreira, H.S.; Matos, G.D.; David, J.M.; Brandão, G.C.; da Silva, E.P.; Portugal, L.A.; Dos Reis, P.S.; Souza, A.S.; et al. Box-Behnken design: An alternative for the optimization of analytical methods. *Anal. Chim. Acta* **2007**, *597*, 179–186. [CrossRef]

37. Yaghoobi, H.; Fereidoon, A. Modeling and optimization of tensile strength and modulus of polypropylene/kenaf fiber biocomposites using Box–Behnken response surface method. *Polym. Compos.* **2018**, *39*, E463–E479. [CrossRef]